Plasma diagnostics of glow discharges in mixtures of CO_2 with noble gases

P.G. Reyes[a], A. Gómez[a], J. Vergara[b], H. Martínez[c], and C. Torres[b]

[a]*Laboratorio de Física Avanzada, Facultad de Ciencias, Universidad Autónoma del Estado de México, Estado de México, 50200, México.*
[b]*Laboratorio de Análisis y Sustentabilidad Ambiental, Escuela de Estudios Superiores de Xalostoc, Universidad Autónoma del Estado de Morelos, Morelos, 62717, México.*
[c]*Laboratorio de Espectroscopia, Instituto de Ciencias Físicas, Universidad Nacional Autónoma de México, Morelos, 62210, México.*

Received 9 January 2017; accepted 18 May 2017

This study presents the plasma diagnostics of a glow discharge produced in two different mixtures, CO_2/He and CO_2/Ar, at a constant pressure of 1.5 Torr. The experiment was conducted to determine the carbon dioxide decomposition in the plasma by using the optical emission spectroscopy (OES) method through identifying lines and emission bands in the spectra. In addition, an electrical characterization of the mixture plasma was made by the determination of ion density (n_i) and the electronic temperature (T_e), estimated through a double Langmuir probe. The electronic temperature for the mixture plasma was in the range of 2.07-5.37 eV, and the ion density between 2.15×10^9 and 18.70×10^9 particles/cm^3. The principal bands and lines identified in the OES correspond to CO_2^+, CO_2, CO^+, CO, O*, O_2, O_2^+, C_2, He* and Ar*.

Keywords: Langmuir probe; electron temperature (T_e); ion density (n_i); OES; gas mixture.

PACS: 52.20.Fs; 52.25.Os

1. Introduction

Plasma is a partially ionized gas, where the electron temperature in the system has values lower than 10 eV with a density of ionized particles in the order of 10^9 particles/cm^3. The species produced in the plasma can interact with each other, producing several species highly reactive in the plasma, with many technological applications [1], such as in semiconductor materials and materials technology (for example, thin film deposition and etching), new light sources, solar cells, water pollution, medical applications, and advanced chemical processes [2–5]. Carbon dioxide (CO_2) is the largest contributor to the greenhouse effect; small variations in the concentration of this gas in the atmosphere can cause adverse effects on the environment and the ecosystem. Therefore, researchers continue to try solving the problems that are caused due to the change in the concentration of CO_2.

In literature, there are several types of studies that show different ways of plasma production to dissociate the molecule of CO_2, which include dielectric barrier discharges, glow discharges, corona discharges, microwave discharges, RF discharges, and the use of mixtures with noble gases such as He and Ar [6]. These noble gases are known to reduce the breakdown voltage in plasmas without changing their properties. For example, in Ar-CO_2 plasma, the presence of Ar helps to sustain the Ar-CO_2 discharge by providing electrons [7], and the energy changes by favoring vibrational processes in the CO_2 molecule before the ionization and then the noble gas can be ionized. Because the Ar ionization potential is much lighter than that of CO_2, the energy loss in the interaction process is reduced; thus, the impinging energy of the electrons increases.

CO_2 is a major source of the greenhouse effect, and no systematic studies on the effect of the He and Ar addition on the CO_2 conversion, including detailed attempts to explain the behavior based on the underlying mechanism, have been reported yet. In the present work, we investigate the effect of He and Ar addition on the CO_2 conversion in a glow discharge over a broad concentration range of He and Ar in the mixture plasma. The decomposition products of CO_2 were analyzed by OES and detailed electrical characterization of the plasma.

2. Experimental Setup

The system that is represented in Fig. 1, described in a previous work [8], comprises two circular electrodes of copper with diameters of 2.5 cm, in a vacuum chamber with a spacing of 20 mm between both electrodes. To evacuate background gases, the chamber (with a volume of 1.16×10^4cm^3) was pumped down to a base pressure of 10^{-6} Torr (turbomolecular pump Alcatel ATP80 and mechanical pump Varian DS302). Subsequently, the chamber was filled with a continuous dynamic flow of CO_2, He, or Ar (ultra-pure gases, Infra 99.99%) through needle valves at the desired pressures. First, the CO_2 gas was introduced in the chamber at a partial pressure, and then, the He (or Ar) gas was introduced in the system. The mixture was varied by changing the partial pressure of He (or Ar) and maintaining a total pressure of 1.5 Torr. Once the plasma was generated, the discharge current values were kept constant at 10 mA, independent of the mixture. The voltage (DC power supply Spellman SA4) was 300 V for 100 % of He, 500 V for 100 % of CO_2 and 270 V for 100% of Ar.

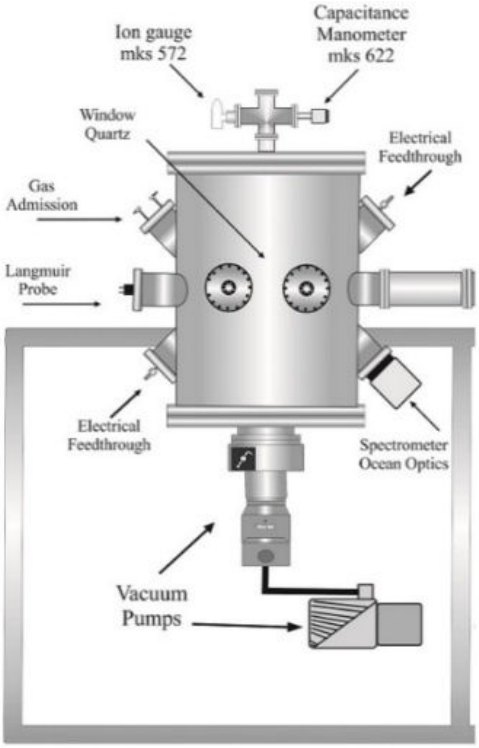

FIGURE 1. Experimental system.

The optical emission spectrum was measured using an Ocean Optics HR4000CG-UV-NIR spectrometer in the range of 200-1100 nm with a resolution of 0.75 nm FWHM. The signal was corrected by considering the spectral sensitivity of the spectrometer. The wavelength accuracy of the spectrometer was calibrated using an Ar source (Ocean Optics Inc.). Spectra data were obtained with a 10 s integration time. Spectral response of the CCD spectrometer was measured using a reference light source (deuterium lamp for UV, and Ocean Optics LS-1-CAL for visible and IR).

With the use of a double Langmuir probe, the electron temperature and ion density were determined. The voltage applied to the probe was provided by a programmable direct current power supply (GW INSTEK, PST-3202), with 1 volt steps, from -30 V to +30 V. The current generated from the collection of charges inside the plasma was measured by a Fluke multimeter. The current-voltage (I-V) curves were the result of an average of 15 data scans.

3. Results

3.1. Optical emission spectroscopy (OES)

3.1.1. CO_2

CO_2^+ is formed through the collision of CO_2 with electrons, photons, and ions/neutral particles or a combination of them, such that they can excite the molecule above its ionization energies. The most common reactions are excitation, ionization, and dissociation.

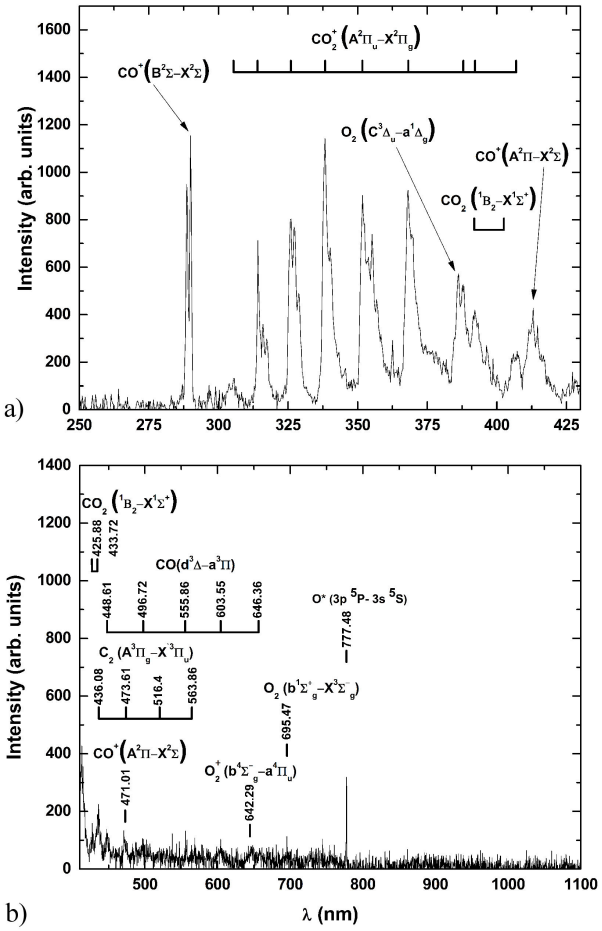

FIGURE 2. a) Optical emission spectrum of CO_2 in the range of 250 to 425 nm. b) Optical emission spectrum of CO_2 in the range of 425 to 1100 nm.

The presence of the First Negative System $\left(B^2\Sigma - X^2\Sigma\right)$ for CO^+, the Chamberlains Airglow System $(C^3\Delta_u - a^1\Delta_g)$ for O_2, the Swan System $\left(A^3\Pi g - X^3\Pi_u\right)$ for C_2, the Triplet Bands $\left(d^3\Delta - a^3\Pi\right)$ for CO, and the FDB System $(A^2\Pi_u - X^2\Pi_g)$ for CO_2^+, among others, is observed in the optical emission spectrum of CO_2, as shown in Fig. 2. The bands identified in the optical emission spectrum of CO_2 are presented in Table I [9, 10]. The spectra related to CO_2 discharge in Fig. 2.a and 2.b is displays in the range of 250 to 425 nm and from 425 to 1100 nm, respectively.

From the identified elements, it can be deduced that the main electronic processes in the plasma of CO_2 are excitation (1) and ionization (2).

$$e^- + CO_2 \rightarrow e^- + CO_2^* \quad (1)$$

$$e^- + CO_2 \rightarrow 2e^- + CO_2^+ \quad (2)$$

The dissociation processes in the molecule of CO_2 generally follows two paths by electron impact [11].

$$e^- + CO_2 \rightarrow e^- + CO{+}O \quad (3)$$

$$e^- + CO_2 \rightarrow e^- + C{+}O_2 \quad (4)$$

TABLE I. Species present in the OES of CO_2.

Species	λ(nm)	Upper configuration	Lower configuration	$v' - v''$
CO^+	289.98	$X^2\Sigma$	$B^2\Sigma$	6,10
CO_2^+	305.66	$X^2\Pi_g$	$A^2\Pi_u$	6,2
CO_2^+	314.16	$X^2\Pi_g$	$A^2\Pi_u$	3,0
CO_2^+	326.09	$X^2\Pi_g$	$A^2\Pi_u$	3, 1a
CO_2^+	338.27	$X^2\Pi_g$	$A^2\Pi_u$	2,0
CO_2^+	351.75	$X^2\Pi_g$	$A^2\Pi_u$	1,1a
CO_2^+	368.11	$X^2\Pi_g$	$A^2\Pi_u$	1,2
O_2	386.27	$a^1\Delta_g$	$C^3\Delta_u$	5,3
CO_2^+	387.53	$X^2\Pi_g$	$A^2\Pi_u$	2,4
CO_2	391.53	$^1B_2$	$X^1\Sigma^+$	-
CO_2^+	392.05	$X^2\Pi_g$	$A^2\Pi_u$	1,1
CO_2	403.08	$^1B_2$	$X^1\Sigma^+$	-
CO_2^+	407.28	$X^2\Pi_g$	$A^2\Pi_u$	1,4
CO^+	413.05	$X^2\Sigma$	$A^2\ \Pi$	1,7
CO_2	425.88	$^1B_2$	$X^1\Sigma^+$	-
CO_2	433.72	$^1B_2$	$X^1\Sigma^+$	-
C_2	436.08	$X^3\Pi_u$	$A^3\ \Pi_g$	4,2
CO	448.61	$a^3\Pi$	$d^3\Delta$	10,2
CO^+	471.01	$X^2\Sigma$	$A^2\Pi$	2,1
C_2	473.61	$X^3\Pi_u$	$A^3\Pi_g$	1,0
CO	496.72	$a^3\Pi$	$d^3\Delta$	6,1
C_2	516.40	$X^3\Pi_u$	$A^3\Pi_g$	0,0
CO	555.86	$a^3\Pi$	$d^3\Delta$	4,1
C_2	563.86	$X^3\Pi_u$	$A^3\Pi_g$	0,1
CO	603.55	$a^3\Pi$	$d^3\Delta$	1,0
O_2^+	642.29	$a^4\Pi_u$	$b^4\Sigma_g^-$	0,1
CO	646.36	$a^3\Pi$	$d^3\Delta$	0,0
O_2	695.47	$X^3\Sigma_g^-$	$b^1\Sigma_g^+$	2,1
O*	777.48	$2s^2 2p^3(^4S^0)3p$	$2s^2 2p^3(^4S^0)3s$	-

Whether the pathway follows (3) or (4) depends on the vibrational excited state of CO_2. It is also possible to observe the presence of the recombination process like carbon (5) and oxygen (6) molecules.

$$C+C \rightarrow C_2 \tag{5}$$

$$O+O \rightarrow O_2 \tag{6}$$

Once formed, CO_2^+ may react in different ways, including any method of CO_2 dissociation already discussed:

$$e^- + CO_2^+ \rightarrow CO_2^* + O \tag{7}$$

$$e^- + CO_2^+ \rightarrow C+ O_2 \tag{8}$$

$$e^- + CO_2^+ \rightarrow CO_2 + hv \tag{9}$$

3.1.2. He

Figure 3 shows the spectrum observed in a He glow discharge. The main electronic process identified is He excitation, which is principally due to electron impact process (Eq. 10).

The energy required to remove the first electron of the He atom is 24.6 eV. The energy for ionization of the He atom is very large; therefore, it is easier to obtain excited levels 3s, 3p, 3d, and 4d because these processes involve less energy consumption.

$$He + e^- \rightarrow He^* + e^- \tag{10}$$

The most intense emission lines of He are listed in Table II.

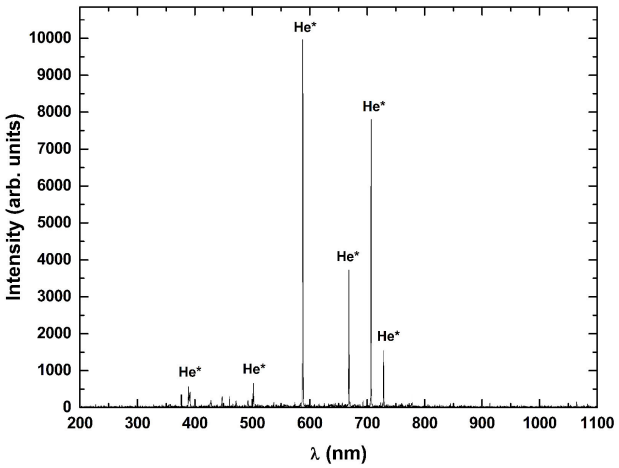

FIGURE 3. Optical emission spectrum of He.

TABLE II. Species present in the OES of He.

Species	λ (nm)	Upper	Lower
He*	389.16	1s3p	1s2s
He*	501.90	1s3p	1s2s
He*	587.69	1s3d	1s2p
He*	668.17	1s3d	1s2p
He*	708.82	1s3s	1s2p
He*	728.44	1s3s	1s2p

3.1.3. *Mixture of CO_2 - He*

Figure 4 displays the optical emission spectrum of the CO_2 -He [33.3% and 66.6%] mixture in two different ranges of wavelengths, from 200 to 500 nm (Fig. 4a) and from 500 to 1100 nm (Fig. 4b), to observe in detail the transition present in the spectra. It is possible to observe small widenings of molecular bands due to vibrational structures. However, when He is added to the CO_2 gas, the effects diminish due to the presence of the following processes

$$\mathrm{He} + e^- \rightarrow \mathrm{He}^+ + 2e^- \tag{11}$$

$$\mathrm{He}^+ + \mathrm{CO_2} \rightarrow \mathrm{CO_2^+} + \mathrm{He} \tag{12}$$

Figure 5(a) displays the OES of the CO_2-He mixture plasma, as a function of He concentrations. It can be observed the presence of CO^+, CO_2^+, O_2, CO_2, CO, C_2 and He species. The intensity of the He* species decreases, while the intensity of the CO^+, CO_2^+, O_2, CO_2, CO, C_2 increases as the He concentration decreases. To understand the effect of the intensity variation of species present in the mixture plasma as a function of the He percentage, we analyzed the evolution of each species as a function of He percentage, by normalizing their intensities (Ix/ΣIx). The line intensity indicates the peak value. Figure 5(b) shows the normalized intensity of CO^+, CO, CO_2, CO_2^+, O_2 C_2 and He species as a function

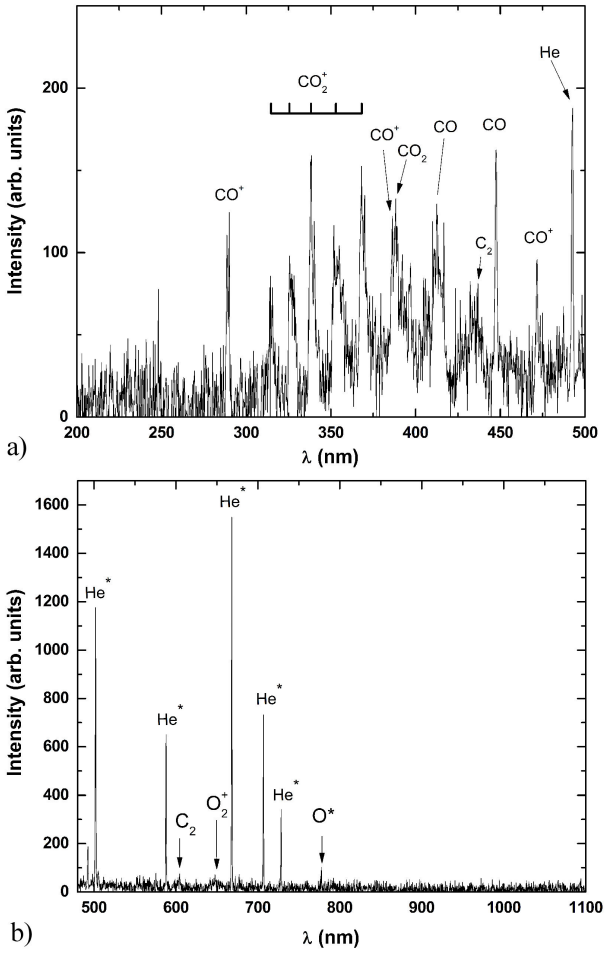

FIGURE 4. 4a) in the range of 200 to 500 nm. 4b): in the range of 500 to 1100 nm. Optical emission spectrum of the mixture CO_2–He [33.3% and 66.6%].

of the He percentage. It was observed that the normalized intensity of the species CO^+, CO_2, CO_2^+, O_2 and C_2 decreases by approximately 56%, while that for CO decreased by 30%, when 33% of He is present in the CO_2-He plasma mixture. Moreover, the intensities of the species coming from CO_2 decrease monotonically as the He concentration increases. CO specie is the most intense in the CO_2-He plasma mixture. This may be because, the ionization and dissociation processes of CO_2 (6.23 eV) are favored because the energy requirement is lower compared to the energy required to excite the Helium atom ($\sim$23 eV).

3.1.4. *Ar*

The Ar emission lines are shown in Fig. 6, which shows that the principal process in the discharge is the atomic excitation by electron impact.

The process of excitation of Ar is described in (13), in which the electron that comes mainly from the plasma interacts with the Ar atom giving sufficient energy to increase its electron levels to 4s and 4p, which are identified with more intensity in OES (Table III).

$$\mathrm{Ar} + \mathrm{e}^- \rightarrow \mathrm{Ar}^* + \mathrm{e}^- \tag{13}$$

TABLE III. Species present in the OES of Ar.

Species	λ(nm)	Upper configuration	Lower configuration
Ar^+	283.00	$3s^2 3p^4(^1D)4p$	$3s^2 3p^4(^3P)4s$
Ar^+	309.00	$3s^2 3p^4(^3P)4d$	$3s^2 3p^4(^3P)4p$
Ar^+	336.50	$3s^2 3p^4(^3P)4d$	$3s^2 3p^4(^3P)4p$
Ar^+	357.00	$3s^2 3p^4(^3P)4d$	$3s^2 3p^4(^3P)4p$
Ar^+	380.00	$3s^2 3p^4(^1D)4d$	$3s^2 3p^4(^1D)4p$
Ar^+	405.00	$3s^2 3p^4(^1S)4p$	$3s^2 3p^4(^1S)4s$
Ar*	416.00	$3s^2 3p^5(^2P_{3/2})5p$	$3s^2 3p^5(^2P_{3/2})4s$
Ar*	420.00	$3s^2 3p^5(^2P_{3/2})5p$	$3s^2 3p^5(^2P_{3/2})4s$
Ar*	427.00	$3s^2 3p^5(^2P_{3/2})5p$	$3s^2 3p^5(^2P_{3/2})4s$
Ar^+	434.50	$3s^2 3p^4(^3P)4p$	$3s^2 3p^4(^3P)4s$
Ar^+	443.50	$3s^2 3p^4(^3P)3d$	$3s^2 3p^4(^3P)$
Ar^+	461.00	$3s^2 3p^4(^1D)4p$	$3s^2 3p^4(^1D)4s$
Ar^+	476.50	$3s^2 3p^4(^3P)4p$	$3s^2 3p^4(^3P)4s$
Ar^+	488.00	$3s^2 3p^4(^3P)4p$	$3s^2 3p^4(^3P)4s$
Ar*	560.50	$3s^2 3p^5(^2P_{3/2})5d$	$3s^2 3p^5(^2P_{3/2})4p$
Ar*	603.50	$3s^2 3p^5(^2P_{3/2})5d$	$33s^2 3p^5(^2P_{3/2})4p$
Ar^+	656.50	$3s^2 3p^4(^3P_2)4f$	$3s^2 3p^4(^1S)3d$
Ar*	675.50	$3s^2 3p^5(^2P_{3/2})4d$	$3s^2 3p^5(^2P_{3/2})4p$
Ar*	696.50	$3s^2 3p^5(^2P_{1/2})4p$	$3s^2 3p^5(^2P_{3/2})4s$
Ar*	706.50	$3s^2 3p^5(^2P_{1/2})4p$	$3s^2 3p^5(^2P_{3/2})4s$
Ar*	727.50	$3s^2 3p^5(^2P_{1/2})4p$	$3s^2 3p^5(^2P_{3/2})4s$
Ar*	738.00	$3s^2 3p^5(^2P_{1/2})4p$	$3s^2 3p^5(^2P_{3/2})4s$
Ar*	750.50	$3s^2 3p^5(^2P_{1/2})4p$	$3s^2 3p^5(^2P_{1/2})4s$
Ar*	763.50	$3s^2 3p^5(^2P_{3/2})4p$	$3s^2 3p^5(^2P_{3/2})4s$
Ar*	772.00	$3s^2 3p^5(^2P_{3/2})4p$	$3s^2 3p^5(^2P_{3/2})4s$
Ar*	794.50	$3s^2 3p^5(^2P_{1/2})4p$	$3s^2 3p^5(^2P_{1/2})4s$
Ar*	801.00	$3s^2 3p^5(^2P_{3/2})4p$	$3s^2 3p^5(^2P_{3/2})4s$
Ar*	811.50	$3s^2 3p^5(^2P_{3/2})4p$	$3s^2 3p^5(^2P_{3/2})4s$
Ar*	826.00	$3s^2 3p^5(^2P_{1/2})4p$	$3s^2 3p^5(^2P_{3/2})4s$
Ar*	842.00	$3s^2 3p^5(^2P_{3/2})4p$	$3s^2 3p^5(^2P_{3/2})4s$
Ar*	852.00	$3s^2 3p^5(^2P_{1/2})4p$	$3s^2 3p^5(^2P_{1/2})4s$
Ar*	912.00	$3s^2 3p^5(^2P_{3/2})4p$	$3s^2 3p^5(^2P_{3/2})4s$
Ar*	922.00	$3s^2 3p^5(^2P_{3/2})4p$	$3s^2 3p^5(^2P_{1/2})4s$
Ar*	965.50	$3s^2 3p^5(^2P_{3/2})4p$	$3s^2 3p^5(^2P_{3/2})4s$

3.1.5. Mixture CO_2/Ar

For Ar, lines of Ar* are observed in the range of 700-850 nm, Fig. 7, as shown in Fig. 7b). By comparing the optical emission spectrum of CO_2 with the spectra of the CO_2-Ar mixtures, a marked decrease is observed in the intensity of the emission bands and CO_2^+ and CO (Fig. 7b).

The presence of CO_2 affects the system configuration, causing changes in the values of electron temperature and the density of ionized particles. When, the molecular gas is introduced into the system, the energy changes, thus favoring the vibrational processes and facilitating the process of Ar ionization [12].

$$Ar + e^- \rightarrow Ar^+ + 2e^- \quad (14)$$

$$Ar^+ + CO_2 \rightarrow CO_2^+ + Ar \quad (15)$$

As the CO_2 concentration increases its percentage in the gas mixture, the intensity of the Ar emission lines in the spec-

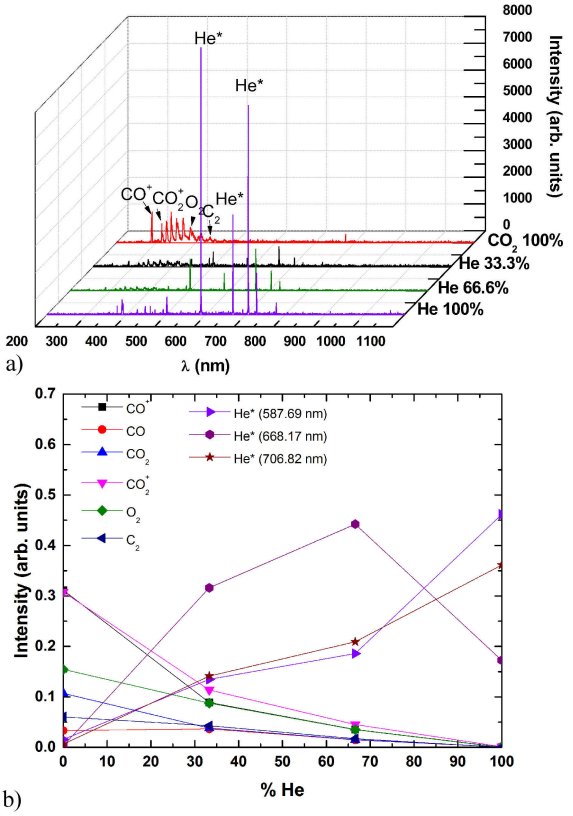

FIGURE 5. a) Optical emission spectra of CO_2-He at different concentrations and; b): Normalized intensity of principal species as a function of He concentration.

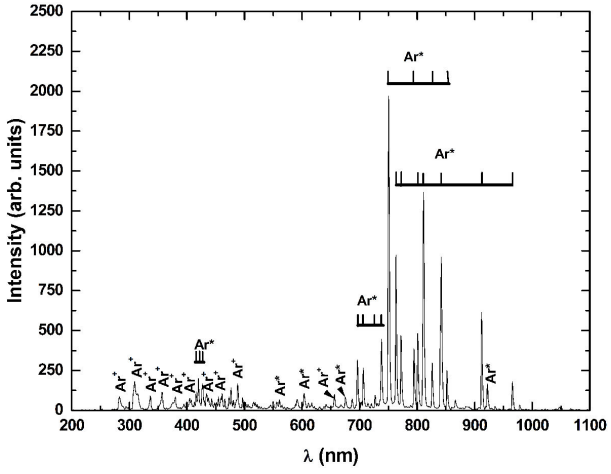

FIGURE 6. Optical emission spectrum of pure Ar.

tra changes, suggesting that the amount of particles of excited Ar also changes. The identified lines for Ar* in the mixture were 696.50, 706.50, 727.50 738.00, 750.50, 763.50, 772.00, 794.50, 801.00, 811.50, 826.00, 842.00 and 912.00 nm. The identification of excited Ar lines is consistent with the amount of energy in the system because it is cold plasma, having at most the interaction process described in Eqs. 14 and 15.

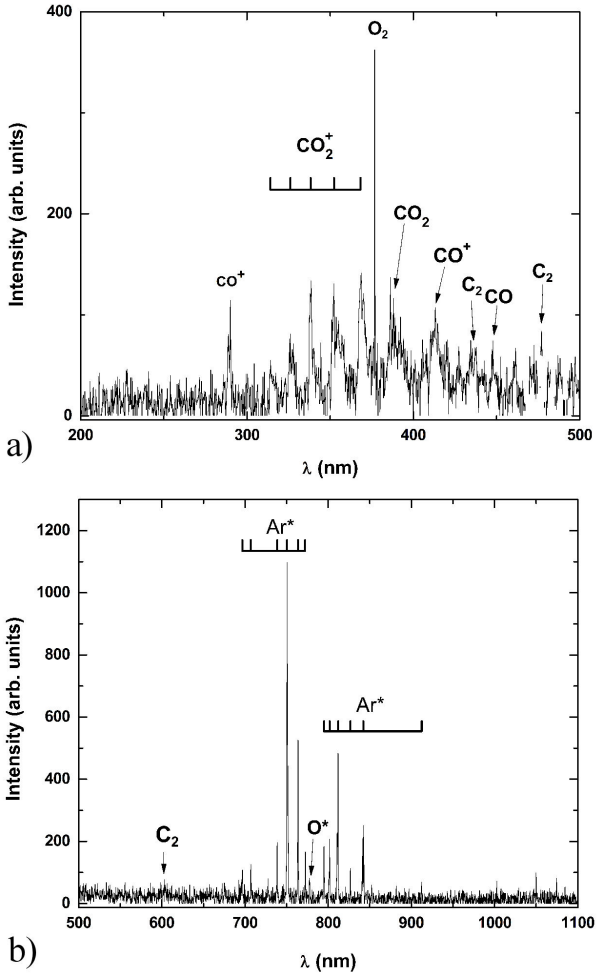

FIGURE 7. a). Optical emission spectrum of the mixture CO_2/Ar [33.3%/66.6%] in the range of 200 to 500 nm; b). in the range of 500 to 1100 nm.

Figure 8a) shows the OES of CO_2-Ar mixture plasma, as a function of the Ar percentage. Figure 8(a) shows the presence of C^+, CO_2^+, O_2, CO_2, CO, C_2, Ar and Ar^+ species. The intensity of the Ar and Ar^+species decreases and the intensity of the CO^+, CO_2^+, O_2, CO_2, CO and C_2 species increases as the Ar concentration decreases. Figure 8b presents the normalized intensities of CO^+, CO, CO_2, CO_2^+, O_2, C_2 and Ar species as a function of the Ar percentage. The emission spectra present a behavior similar to the CO_2-He plasma mixture case. That maybe due to the energy requirement to ionize or excite the Ar atom (∼15.76 and 11.55 eV respectively) are bigger than the CO_2 molecule, like the CO_2-He plasma mixture case.

The energy in the system is favorable to have the presence of the process of dissociation of the molecule of CO_2, mainly due to electronic processes through electron impact. The intensity ratio of CO-CO_2 mixtures plasma (Fig. 9) shows that the dissociative effect for electron impact increases with the presence of some noble gases being more efficient for He in this work, however the ratios between the intensities belonging to the molecular O_2 and CO_2, Fig. 10, remain close,

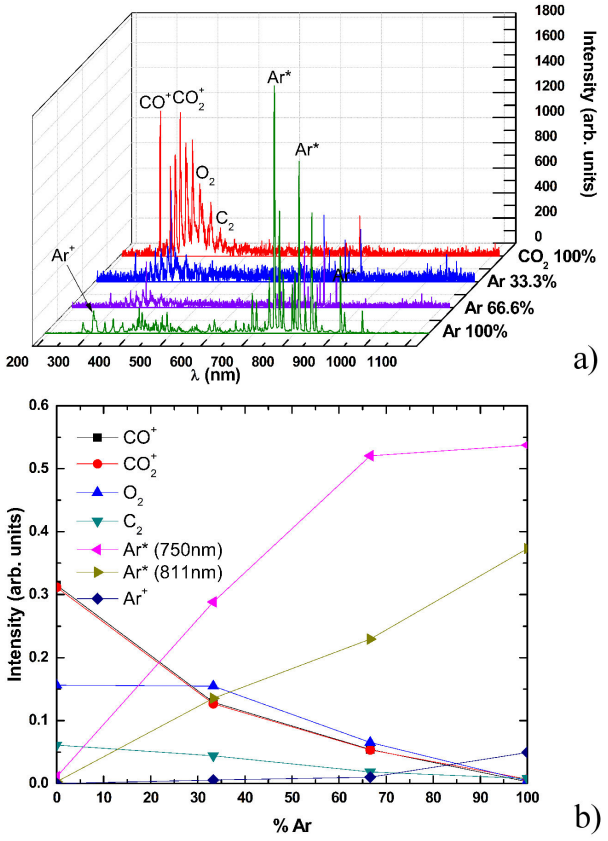

FIGURE 8. a): OES of CO_2-Ar at different concentrations; b): Normalized intensity as a function of Ar concentration.

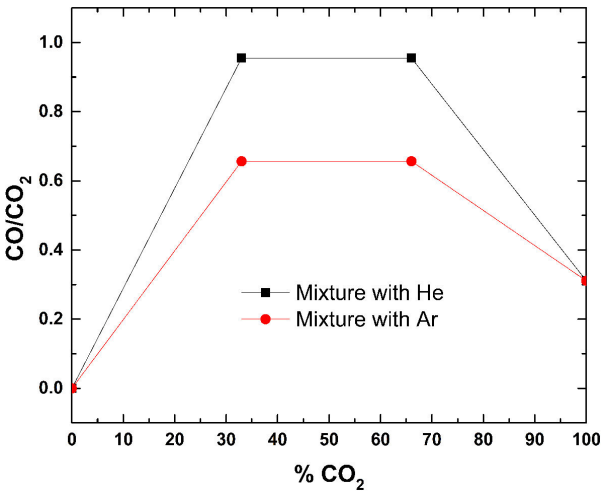

FIGURE 9. The intensity ratio of CO-CO_2 in mixture with Ar and He.

which means that the O_2 production rate are constant, independently of the noble gas used in the mixture plasma. Secondly, due to values ratios for O_2 being greater than O_2 compared with those of CO_2, it is evident that the O_2 production is more efficient for both gas, *i.e.* Ar and He. Thus the path dissociation established in the Eq. 4 is favored in both cases, the dissociation process is more important than the excitation.

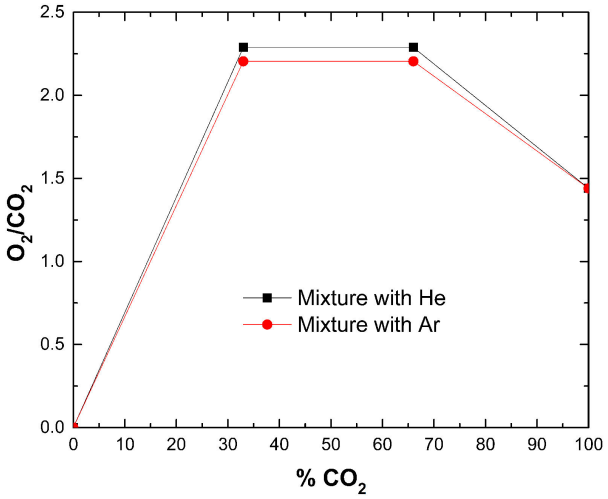

FIGURE 10. The intensity ratio of O_2-CO_2 in mixture with Ar and He.

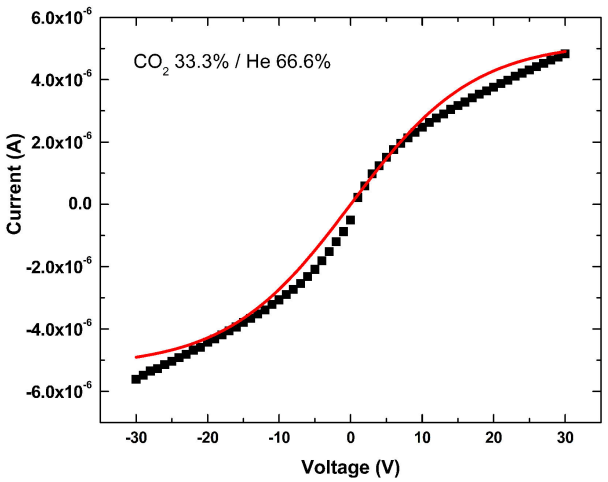

FIGURE 11. Curve fit of double Langmuir curve of V vs. I.

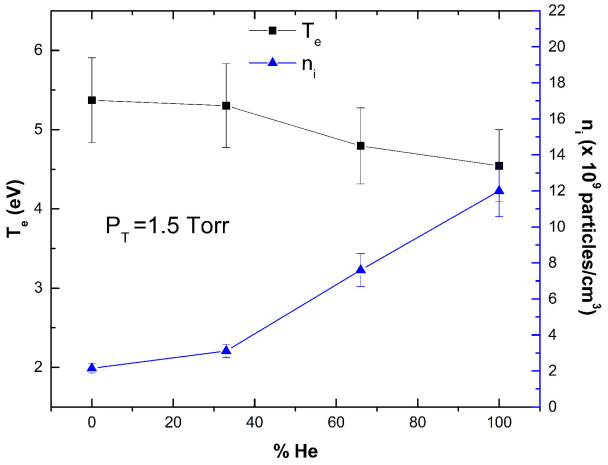

FIGURE 12. T_e and n_i in a mixture of CO_2-He at different concentrations of He.

3.2. Electrical characterization

3.2.1. *Double Langmuir probe, electron temperature, and ion density*

Figure 11 shows the I-V characteristic curve of the 33.3% CO_2-66.6% He mixture plasma, obtained by the double Langmuir probe, along with the corresponding theoretical curve (solid curve). The evaluation of electron temperature (T_e) and ion density (n_i) runs in the following way; first, the probe characteristic curve is differentiated two times. The electron temperature is calculated through the position of the extrema of the characteristic curve's second derivative [13]. Then a theoretical curve is fitted to the entire measured experimental I-V characteristic curve by adjusting only the ion density. This evaluation procedure gave an electron temperature of T_e and an ion density of n_i, at each mixture plasma used in this work.

The electronic temperature (T_e) of the mixture is in the range of 4.54 to 5.37 eV, and the ion density (n_i) has values between 2.15×10^9 and 12.00×10^9 particles/cm^3. The behavior of the aforementioned values is shown in Fig. 12, for different He concentrations. In this work, from ten measurements, the overall variation in the electron temperature and the ion density were found to be 10%.

Performing a similar procedure to obtain the electrical characterization make for before Ar and CO_2-Ar plasmas. In Fig. 13 characteristic (I-V) double Langmuir curve is shows. The electron temperature (T_e) values are in the range of 2.07 to 5.37 eV, and the ion density (n_i) values are between 1.87×10^{10} and 2.15×10^9 particles/cm^3 (Fig. 14). With the addition of Ar gas in the plasma, there is an increase in electron density, which leads to a high electron-electron collision frequency and always tends to deplete electrons. Thus, a decrease in the electronic temperature is caused.

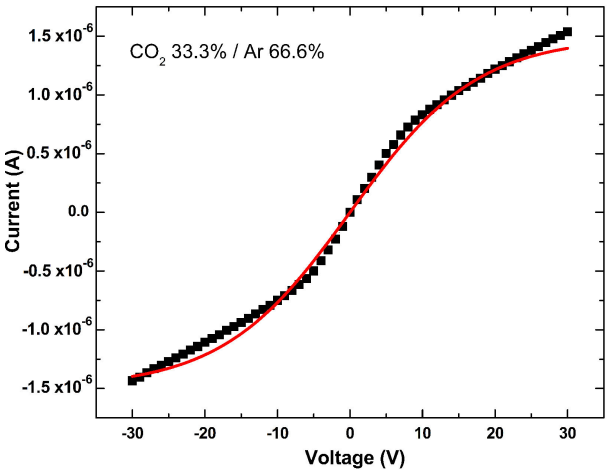

FIGURE 13. I vs. V characteristic curve for CO_2-Ar.

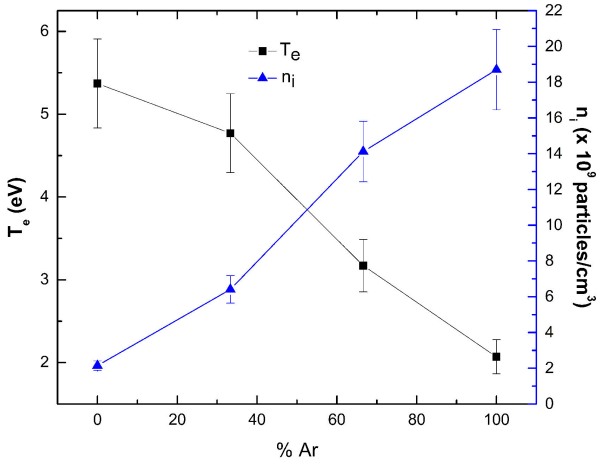

FIGURE 14. T_e and ni in a mixture of CO_2/Ar at different concentrations of Ar.

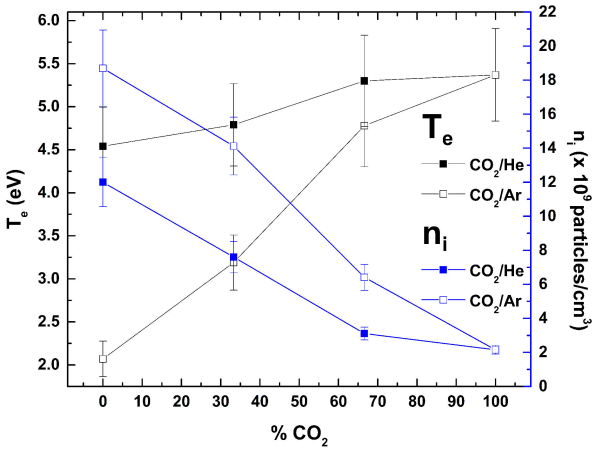

FIGURE 15. T_e and n_i in mixtures of CO_2-He and CO_2-Ar at different concentrations of CO_2.

Figure 15 shows the observed behavior of the variables obtained by the electric Langmuir probe, electron temperature, and ion density, as a function of the percentage of molecular gas CO_2 present in the mixture.

Figure 15 also shows the behavior of the electron temperature and ion density as a function of the percentage of CO_2 in the mixture for both Ar-CO_2 and He-CO_2 mixtures plasma. Both behaviors are similar, the electron temperature

TABLE IV. Values of T_e and n_i for CO_2-He and CO_2-Ar mixtures.

	CO_2-He		CO_2 -Ar	
% CO_2	T_e (eV)	n_i ($\times 10^9$ particles/cm^3)	T_e (eV)	n_i ($\times 10^9$ particles/cm^3)
0	4.54	12.00	2.07	18.70
33.3	4.79	7.60	3.19	14.12
66.6	5.30	3.11	4.78	6.41
100	5.37	2.15	5.37	2.15

decreases, while the ion density increases as the concentration of the noble gas increases. Besides, we can observe that with the addition of Ar, the ion density and electron temperature increased more as compared to when He was added.

The values of T_e and n_i in the mixture are present in Table IV.

4. Conclusions

A detailed OES and electrical characterization of glow discharges operating in CO_2, and CO_2-He and CO_2-Ar mixtures to investigate the CO_2 decomposition were performed. When, CO_2 gas is mixed with a noble gas (Ar or He), the average kinetic energy of electrons decreases, while the amount of ionized particles increases. This effect can be explained by the fact that the concentration of a noble gas in the mixture increases, as the electron collisional frequency decreases, causing the electrons to be in the presence of an electric field longer, which accelerates them.

According to the analysis of the normalization intensities and, CO-CO_2 and O_2-CO_2 ratios obtained by an OES, the intensity of the decomposition products of CO_2 in the mixture of CO_2-He is greater than CO_2-Ar mixture at the same concentrations. This is consistent with the studies of these mixtures conducted with different experimental techniques to produce the plasma. CO_2 could be efficiently decomposed by glow discharge of CO_2-He and CO_2-Ar mixtures. He gas was found to be more effective for the preferential decomposition of CO_2 of CO + O at a 33% Ar/66% CO_2 mixture.

The electron temperature was found to be in the range of 2.07 to 5.37 eV, and the ion density was between 2.15×10^9 and 18.70×10^9 particles/cm^3. The species identified were CO_2^+ resulting from $CO_2 + e^- \rightarrow CO_2^+ + 2e^-$; CO^+ resulting from $CO_2 + e^- \rightarrow CO^+ + O + 2e^-$; CO resulting from $CO_2 + e^- \rightarrow$ CO+O+e$^-$, and O* resulting from O+O $\rightarrow O_2, O_2^+$ resulting from $CO_2 +$ e$^-$ $\rightarrow$ C+O_2++2e$^-$, and C_2 resulting from C+C $\rightarrow C_2$. whereas the noble gases emission lines identified were He* and Ar*.

Acknowledgments

We are grateful to O. Flores (ICF-UNAM) for her technical assistance. This research was supported by DGAPA [IN-102916], CONACyT [268644], PROMEP [103.5/13/6626], PRODEP [DSA/103.5/15/6986], PII-43/PIDE/2013 and UAEM 4307/2017/CI.

1. A. Bogaerts, T. Kozak, K. van Laer, R. Snoeckx, *Faraday Discuss.* **183** (2015) 217.
2. A. Bogaerts, E. Neyts, R. Gijbels, J. van der Mullen, *Acta Part B* **57** (2002) 609.
3. R. Kenneth Marcus, *Glow discharge spectroscopies*, 1st edition (Springer Science+Business Media New York, NY, 1993) 1-3.
4. R. Payling, D. Jones, A. Bengtson, *Glow Discharge Optical Emission Spectrometry*, 1st edition (Wiley, Michigan, 2010) 38.
5. R. Kenneth Marcus, J.A. C. Broekaert, *Glow Discharge Plasmas in Analytical Spectroscopy*, (John Wiley Sons, England, 2003). p. 1-3.
6. Danhua Mei, Xinbo Zhu, Ya-Ling He, Joseph D Yan and Xin Tu, *Plasma Sources Sci. Technol.* **24** (2015) 1.
7. Spencer L., Thesis of Doctor of Philosophy: *The Study of CO_2 Conversion in a Microwave Plasma/Catalyst System*, (University of Michigan, 2012) 1.
8. J. Torres, P. Guillermo Reyes; C. Torres, H. Martiínez, J. Vergara, *IEEE Transactions on Plasma Sciences* **43** (2015) 846.
9. NIST, http://www.nist.gov/index.html
10. R.W.B. Pearse *The identification of molecular spectra*, Chapman and Hall Ltd, USA, (1976) 116-118. S.L. Brock, Manuel Marquez, Steven L. Suib, Yuji Hayashi, Hiroshige Matsumoto, *Plasma Decomposition of CO_2 in the Presence of Metal Catalysts*, *Journal of Catalysis*, **180** (1998) 225.
11. S.L. Brock, M. Marquez, S.L. Suib, Yuji Hayashi, *Journal of Catalysis* **180** (1998) 225.
12. L.F. Spencer and A.D. Gallimore *Plasma Sources Sci. Technol.* **22** (2013) 015019.
13. E.F. Mendez-Martinez, P.G. Reyes, D. Osorio- Gonzalez, F. Castillo and H. Martinez, *Plasma Sci. Technol*. **12** (2012) 314.